

NUMERICAL ESTIMATES OF THE ATMOSPHERIC INFLUENCE ON THE SIGNAL SHAPE IN SENSING SEA WATER

G.M. Krekov, M.M. Krekova, and V.S. Shamanaev

*Institute of Atmospheric Optics,
Siberian Branch of the Russian Academy of Sciences, Tomsk
Received October 10, 1992*

The results calculated for $\lambda = 0.53 \mu\text{m}$ by the Monte Carlo method are presented. This makes it possible to estimate the influence of the atmosphere on the shape of signals obtained with the help of an airborne lidar from sea water. Analysis of results shows that a limiting effect of the atmosphere on the maximum depth of sounding is possible under specific optical conditions and experimental geometry.

High efficiency of airborne systems in application to oceanological and ecological studies is, at present, quite obvious. Data on the medium state can be extracted from the time characteristics of an echo signal. Interpretation of the results is quite a difficult problem itself, because sea water is a multicomponent medium. The distortion of the time characteristics of a signal occurs due to the effects of the multiple interaction of radiation with scattering and absorbing particles. Moreover, the pulse shape can additionally be modified due to the atmospheric scattering and interaction with the air–water interface when using airborne sounding systems.

Nonstationary character of the interface under the wind–driven sea waves results in an increase of the effects of reflection and rereflection of radiation scattered by the atmosphere. Low optical density of the atmospheric layer elevates the accumulation of large free paths of photons, i.e., signals from underwater $P_w(t)$ and from the air–water interface $P_a(t)$ reach the receiver simultaneously. In Refs. 1–3 it was pointed out that the atmosphere influences the formation of the echo signal coming from the boundary water layer. A delay of the decrease of sounding signal $P_w(t)$ starting from a certain depth was observed during the experiment in Ref. 1. Levin and Feigels³ explained this effect by the presence of the signal $P_a(t)$, in addition, they proposed an approximate analytical expression for estimating $P_a(t)$.

When planning and carrying out lidar measurements account must be taken of the above–indicated effect, in this connection it is necessary to study it in more detail. We think that the numerical simulation should be performed for determining the role of different factors in the formation of the signal $P_a(t)$ as well as for estimating the optical conditions and experimental geometry under which the atmospheric signal can limit the depth of sensing into sea water.

The most complete data on the atmospheric component of the lidar return can be obtained from the solution of the radiative transfer equation under certain boundary conditions. Such a solution is normally sought for by the Monte Carlo method.

A monostatic lidar was assumed to be removed from a rough sea surface at a distance H . At the height h , there is an interface, which is represented as a set of randomly oriented microareas whose centers lie in the plane $z = h$, while $\mathbf{S} = \{S_x, S_y, S_z\}$ are the normals to these areas whose probability density distribution $P(\mathbf{S})$ is a truncated two–dimensional probability density distribution of slopes z_x and z_y (Ref. 4).

$$P(\mathbf{S}) = 2\pi(\sigma_x\sigma_y)^{-1} \exp\{-(z_x/\sigma_x)^2/2 - (z_y/\sigma_y)^2/2\},$$

where the variances of slopes are $\sigma_x^2 = 0.00316V$, $\sigma_y^2 = 0.003 + 0.00192V$, and V is the wind velocity [m/s].

The atmospheric signal can be determined by two components: by radiation scattered by aerosols and radiation reflected from the interface. In complex solution of the problem in the ocean–atmosphere system the signal can be underestimated due to a small optical density of the atmospheric layer. The peculiarity of the method is that the statistics, being essential for estimating the signal $P_w(t)$, is not the same as for $P_a(t)$. Therefore, the problem was solved by two stages. At the first stage with high statistics, only the atmospheric signal was estimated while the trajectories of photons, which were subjected to refraction at the interface and then pass to the deep water layers, were broken off and removed from further consideration. This made it possible to estimate the temporal dependence $P_a(t)$ at large time and for a large number of reception angles. At the second stage, the solution for the signal component $P_w(t)$ was performed taking into account all the complex of lidar operation conditions. Thus, the history of the photon trajectory was completely built starting from the source but the probability of the photon to reach the receiver was estimated only when the photon was scattered by a hydrosol particle. It should be noted that the method of local estimate⁵ was applied to the construction of the algorithms.

The radiation power averaged over space or ensemble of realizations was estimated as a result of the solution. Detailed description of the theory and mathematical statement of this problem was considered in Refs. 5 and 6. Let us note only that calculations were performed for $\lambda = 0.53 \mu\text{m}$ for a point source emitting almost instantaneously $\delta(t - t^0)$ the light signal whose energy is distributed over a solid angle Ω_s with the divergence angle of the source φ_s . The reflected signal was recorded within the solid angle Ω_r with the angle of the receiver field of view φ_r . The angle $0.5 \varphi_s$ was equal to 1 mrad while the angle φ_r varied within the limits $1 \text{ mrad} \leq \varphi_r \leq 0.35 \text{ mrad}$.

Optical properties of the atmosphere over the ocean were taken in accordance with Deirmenjian's M haze model while the extinction coefficient σ_a was varied from 0.2 to 0.4 km^{-1} . The extinction coefficient of sea water was determined by the additive components caused by scattering and absorption by water, suspended particles, and dissolved

organic components. For the open ocean σ_w was taken to be 0.2 m^{-1} and the absorption was taken into account by the probability of photon survival $W = 0.81$, while σ_w for coastal water was equal to 0.4 m^{-1} and $W = 0.87$. Scattering phase functions with their mean cosine $\langle \cos \mu \rangle = 0.95$ for the open ocean and $\langle \cos \mu \rangle = 0.8$ for coastal waters were used in calculations. The sea surface was estimated for the wind velocity V varying from 1 to 7 m/s.

Before proceeding to the discussion of the results we should like to note that calculations were performed with large statistics using an "El'brus" computer complex, the statistical data bulk was equal to 4 million photon histories for the aerosol layer and 500 000 – for water.

Figure 1 shows the calculated results on the time dependence of the additive components of the echo signal $P(t)$. The signal $P_w(t)$ from water is shown by curves 1–3 and the atmospheric component of the signal $P_a(t)$ is shown by curves 1'–3', the latter is given starting from the point of

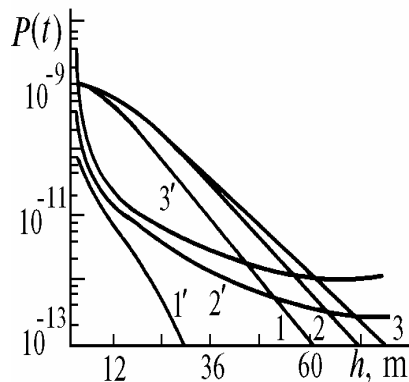


FIG. 1. Time dependences of the signal components, curves 1–3 are for $P_w(t)$ and 1'–3' for $P_a(t)$ at $0.5 \varphi_r = 1, 5, \text{ and } 10^\circ$, respectively, $V = 1 \text{ m/s}$.

Taking into account the above-mentioned considerations very wide angles of the receiving field of view $0.5\varphi_r \geq 2\text{--}3^\circ$ are not advisable to be used in sensing of the upper layer of water with the purpose of obtaining data on its optical properties. In addition, under conditions of wind-driven sea waves the energy of the receiving signal at the angles $0.5\varphi_r \sim 1^\circ$ is close to maximum.⁶

Data presented in Fig. 2 show the results of a more detailed analysis of the formation $P_a(t)$. The component $P_a(t)$ comprising the multiply scattered radiation by aerosols in the processes of reflection and rereflection from the interface is shown by dashed curve. Calculations performed with the separation of interactions of different multiplicities show that the processes of rereflection are nonessential in the formation of $P_a(t)$. The atmospheric component is first of all formed by multiply scattered radiation and its participation in the process of primary reflection. Low optical density of the atmosphere and a weak asymmetry of the scattering phase function make favorable conditions for accumulating large free paths of photons (even at low multiplicities of scattering) and maintaining sufficiently stable level $P_a(t)$ up to a long time.

The effect of variations of the interface state occurring due to the wind action on the shape of $P(t)$ is illustrated by the data presented in Fig. 3. The figure shows the time

the corresponding time of the radiation arrival from the boundary water layer. Calculations are shown at three reception angles in the limits $1^\circ < 0.5\varphi_r < 10^\circ$. At reception angles $0.5\varphi_r \leq 1^\circ$ the atmospheric component of the signal is of no practical importance within the considered time interval, i.e., its level is several orders of magnitude lower than the level of $P_w(t)$.

Calculations show that starting only from the angles of receiver field of view $0.5\varphi_r \geq 3^\circ$ the time characteristic $P_a(t)$ intersects $P_w(t)$. At $0.5\varphi_r \sim 3^\circ$ this intersection occurs at the depth about 80 m and with increase of the reception aperture $0.5\varphi_r$ up to 10° it shifts upward to the water layers about 50–60 m. Moreover, high level of $P_a(t)$ with respect to $P_w(t)$ was observed in the signal coming from 2–4 m water boundary layers. Such a ratio of signal levels is formed due to a primary reflection of the photons previously singly scattered by the atmosphere and can be observed at the sufficiently wide receiving apertures $0.5\varphi_r \geq 5^\circ$.

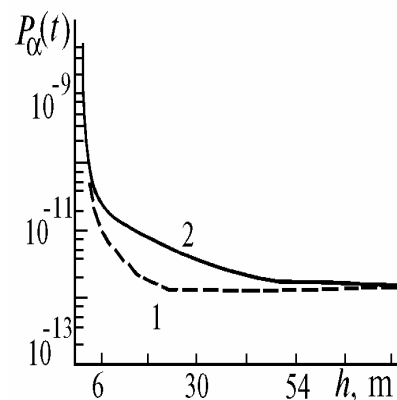


FIG. 2. The atmospheric component $P_a(t)$ of a lidar return: curve 2 is for $P_a(t)$ and curve 1 is for $P_a(t)$ caused by the reflection and rereflection processes. Calculation is performed at $0.5\varphi_r = 10^\circ$.

dependence of the ratio $P_a(t)/P(t)$, where $P(t) = P_w(t) + P_a(t)$, characterizing the contribution of the atmospheric component of a signal into the total signal.

As is shown in Ref. 7 the energy of the signal coming from the boundary layer of water decreases with increase of the wind velocity. The absolute level $P_w(t)$ decreases as well. It is obvious, therefore, that the relative contribution of $P_a(t)$ into $P(t)$ slightly increases with increase of wind velocity. The dependence of the ratio $P_a(t)/P(t)$ on V virtually disappears at large t . The same regularity is also observed in the behavior of $P_w(t)$ (see Ref. 7). Obviously, the character of the behavior $P_a(t)/P(t)$ depends on both components $P_a(t)$ and $P_w(t)$. Calculations show that the absolute level of $P_a(t)$ decreases with increase of the wind velocity. The mechanism of formation of $P_a(t)$ is quite complicated in the presence of the nonstationary interface. On the one hand, a certain portion of photons leaves the limits of the receiving field of view due to reflection of directly unscattered radiation, the process strengthens with increasing wind velocity. On the other hand, a portion of multiply scattered and reflected radiation, which occurs at the periphery of a beam, returns again into the observation angle after reflections and rereflections. But the first tendency dominates, and as a result the absolute level $P_a(t)$ decreases with increasing wind velocity.

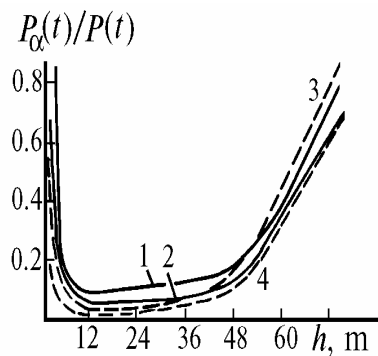


FIG. 3. Time dependence of the relative contribution $P_a(t)$ into $P(t)$. Curves 2 and 4 are calculated at $0.5\varphi_r = 5^\circ$ while curves 1 and 3 — at $0.5\varphi_r = 10^\circ$. Solid curves are for $V = 1$ m/s and dashed curves are for $V = 7$ m/s.

Figure 4 shows the results of the effect of the variation in the optical state of the atmosphere on the ratio $P_a(t)/P(t)$. An increase in the atmospheric optical density by a factor of two results in the fact that the level $P_a(t)$ becomes comparable with $P_w(t)$ as low as at the depth of 50 m and then exceeds it. The signal coming from the 70–80 m depth to the receiver with $0.5\varphi_r > 5^\circ$ can be virtually completely determined by the atmospheric component. An increase in the optical density of sea water causes a decrease of the relative contribution of the atmospheric component into the signal $P(t)$. Calculations were performed for $\sigma_w = 0.4$ m⁻¹ and $W = 0.87$ for the water layer $\Delta h = 50$ m. Over all time interval, i.e., up to the depth 50 m, $P_w(t) \gg P_a(t)$. That is connected with the presence of high level of the background within the receiving aperture $0.5\varphi_r \geq 5^\circ$.

The above calculations were performed with the scattering phase function typical of the open oceans. The scattering phase functions of coastal water are characterized by a less asymmetry and by an increase of scattering within the range of sounding angles.

Calculations performed for this type of water (see Fig. 5) show that the relative contribution $P_a(t)$ into a signal is negligible. There are virtually no limitations related to the effect of the atmosphere at small t , they are observed only in the sounded water layers at about 70 m. It should be noted that the depth of sounding of coastal water is limited by its optical density.

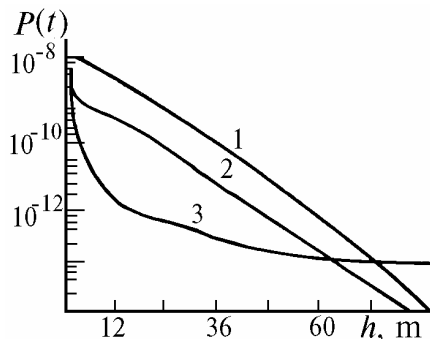


FIG. 5. The lidar return $P_w(t)$ calculated for two scattering phase functions: 1) open ocean, 2) coastal water, and 3) $P_a(t)$ for $\sigma_a = 0.2$ km⁻¹. Data are calculated for the angle $0.5\varphi_r = 10^\circ$.

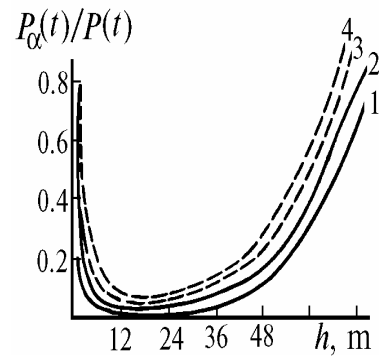


FIG. 4. The ratio $P_a(t)/P(t)$ at two atmospheric states. Solid curves are for $\sigma_a = 0.2$ km⁻¹ and dashed curves are for $\sigma_a = 0.4$ km⁻¹, curves 1, 3 and 2, 4 are for $0.5\varphi_r = 5^\circ$ and 10° , respectively.

Thus, the analysis of the results of numerical simulations show that a limitation on the sounded depth caused by the atmospheric effect is observed at large angular receiving apertures, for example, at $H = 200$ m the angles of receiving field of view are $0.5\varphi_r \sim 3\text{--}5^\circ$ while with increase in the distance H they are proportionally decreasing. A decrease of the receiving aperture down to $0.5\varphi_r \leq 1^\circ$ removes limitations almost at any t , however, the absolute level of the sounding signal becomes lower and its dynamic range wider. This is connected with a sharp decrease in the level of the background component of the signal coming from the deep water layers.

The obtained results allow one to state that obviously the anticipated depths of sounding⁷⁻⁹ up to 8–15 typical lengths (of the order of 150 m and more) cannot be reached. The signal coming to the receiver from the depths of the order of 100 m is, in fact, almost the atmospheric one. Its dominating role, starting from 50–70 m (depending on optical conditions and experimental geometry) can be seen in the stability of the behavior $P(t)$, the level of the signal quite slowly decreases with increase of the observation time.

REFERENCES

1. F.E. Hoge, R.N. Swift, and E.B. Frederick, *Appl. Opt.* **19**, No. 6, 871 (1980).
2. F.E. Hoge, C.W. Wright, W.B. Krabil, et al., *Appl. Opt.* **27**, No. 19, 3969 (1988).
3. I.M. Levin and V.I. Feigel's, in: *Optics of the Sea and Atmosphere*, L.V. Kirenski Institute of Physics, Siberian Branch of the Academy of Sciences of the USSR, Krasnoyarsk (1990), Part 2, pp. 64–65.
4. C. Cox and W. Munk, *J. Opt. Soc. Am.* **44**, No. 11, 838 (1957).
5. G.I. Marchuk, G.A. Mikhailov, et al., *The Monte Carlo Method in Atmospheric Optics* (Springer, Berlin, 1980).
6. E.O. Dzhetysbaev and B.A. Kargin in: *Current Problems of Applied Mathematics and Numerical Simulation* (Nauka, Novosibirsk, 1982), 83 pp.
7. B.A. Kargin, G.M. Krekov, and M.M. Krekova, *Atm. Opt.* **5**, No. 3, 191–195 (1992).
8. C.A. Lewis, W.G. Swamer, et al., in: *Abstracts of Reports at NASA Conference on Use of Lasers for Hydrographic Studies*, NASA Sp-375, 67 (1973).
9. G.D. Hicman in: *Abstracts of Reports at NASA Conference on Use of Lasers for Hydrographic Studies*, NASA Sp-375 (1973), p. 67.
10. D.A. Vlasov, *Izv. Vyssh. Uchebn. Zaved. Akad. Nauk SSSR, Ser. Fiz.* **49**, No. 3, 433–441 (1985).